Sedimentary Rocks of Early Mars

Michael C. Malin* and Kenneth S. Edgett

Layered and massive outcrops on Mars, some as thick as 4 kilometers, display the geomorphic attributes and stratigraphic relations of sedimentary rock. Repeated beds in some locations imply a dynamic depositional environment during early martian history. Subaerial (such as eolian, impact, and volcaniclastic) and subaqueous processes may have contributed to the formation of the layers. Affinity for impact craters suggests dominance of lacustrine deposition; alternatively, the materials were deposited in a dry, subaerial setting in which atmospheric density, and variations thereof mimic a subaqueous depositional environment. The source regions and transport paths for the materials are not preserved.

Deciphering the geologic history of Mars is today one of the most important areas of research in space science. In addition to the intrinsic interest in understanding how planets evolve and how Mars specifically came to be the way it is, the geology also provides the foundation upon which many other areas of inquiry are based. The Mars Global Surveyor (MGS) Mars Orbiter Camera (MOC) (*1*) was designed to test hypotheses about martian geology that had been proposed on the basis of the Mariner and Viking data gathered in the 1960s and 1970s. Among these hypotheses are those that center on what the planet was like during its earliest years (before 3.5 billion years ago), the Noachian Period (*2*), and what the planet was like in more recent times, the Amazonian Period. One of the primary questions about the Noachian is whether it was warmer and wetter than the cold, arid Mars we see today, such that liquid water could persist on its surface for thousands to millions of years (*3*, *4*). A key question regarding the Amazonian is whether there were climate excursions after the present cold and dry conditions were established that again allowed liquid water to persist on the surface long enough for lakes or seas to have occupied the chasms of the Valles Marineris and many impact craters around the planet (*5*–*9*). Speculative affirmative answers to both of these questions are widely cited as indicators that Mars may have had conditions favorable to the development and persistence of life (*10*–*12*). In this paper, we present geologic evidence that these two hypotheses are linked—that the materials in craters and chasms considered for two decades to be Amazonian in age were instead formed in the Noachian, that there are many more outcrops of these materials than previously known, that they could indeed represent sediment deposited in lakes, and that they are a small part of a substantially more complex, previously unanticipated, martian history.

Malin Space Science Systems, Post Office Box 910148, San Diego, CA 92191–0148, USA.

*To whom correspondence should be addressed.

Figure 1 shows a series of cliff-forming, light-toned layered outcrops (*13*) located in chasms and craters distributed across, and in some cases separated by, thousands of kilometers at equatorial latitudes on Mars. Each image shows eroded, layered materials of similar thickness, relative brightness, and morphologic expression. A few of these examples—particularly in the Valles Marineris troughs (Fig. 1, A, B, E, and F)—have been known since the Mariner 9 mission but were not seen with the detail obtained by the MOC. The others were not previously known, and hundreds of additional, similarly layered outcrops have been detected (Fig. 2). These outcrops are limited to specific regions and settings on Mars, and are distinct from much of the rest of martian terrain, which is covered by dunes, dust mantles (*14*), rugged meter-scale relief, and/or small impact craters.

Outcrop Observations

Outcrops occurring at the locations noted in Fig. 2 are divided into three classes of unit (*15*)—layered, massive, and thin mesa—based on visual tone (Fig. 3A) (*16*), thickness (Fig. 3B) (*17*), texture, and configuration (*18*). This classification is intended to facilitate communication by grouping features of similar properties, but is not intended to imply lateral and/or stratigraphic continuity from place to place on Mars (*19*). Individual outcrop sites usually include more than one of the three unit types, and substantial diversity is often well expressed within each type at any given location.

"Layered" units are light- to intermediate-toned; thin (a few meters to ~200 m) to thick (~200 to 2000 m); and contain one to hundreds of thin, tabular sub-units, or "beds" (Figs. 3B and 4). Beds in layered units are sufficiently thick to be observed at the scale of the highest resolution MOC images (1.5 to 6.0 m/pixel). Distinctive forms include stair-stepped (extremely regular and repetitive bedding with nearly uniform thickness) (Fig. 4A), cliff-bench (bedding with well-marked vertical and horizontal expression but not as regular and uniform as stair-stepped) (Fig. 4, B, C, and D), and banded (bedding characterized primarily by brightness differences) (Fig. 4E). In some places, particularly in Arabia Terra craters such as Henry (Fig. 4F), layer albedo is muted or obscured by light-toned mantles.

"Massive" units are light- to intermediate-toned, hundreds of meters to a few kilometers thick, not layered or poorly bedded, and, in some locales, include forms that are transitional from layered to massive. In the few examples where seen together, well-bedded layered units appear at the base of the section and below the massive unit (Fig. 3B). The transition from layered to massive units may be gradational or abrupt, but is easily characterized by a distinct change in surface morphology, from cliffs and benches that are approximately parallel to topographic contours to ridges and furrows oriented up- and down-slope. In some locales, the ridges and furrows are more accentuated at specific topographic positions within the massive unit, suggesting gross layering (*20*). Massive units are most common within the Valles Marineris troughs, particularly Hebes, Ganges, Ophir, and Candor chasms.

"Thin mesa" units usually consist of dark- or occasionally intermediate-toned, thin, mesa-forming (and, in some places, resistant caprock–forming) materials. These units are found nearly everywhere that layered and/or massive units occur, and they have surfaces that vary from relatively smooth to pitted to intensely ridged and grooved (Fig. 5). Thin mesa units almost always lie unconformably over previously eroded massive and/or layered units. This relation is best seen on slopes where layered units are exposed and thin mesa units drape across the beds (Fig. 5D). The ridged-and-grooved textures of some thin mesa units resemble eolian bedforms (Fig. 5C), but their sharply delineated occurrence only within the boundaries of the mesa-forming units, sharp crests and symmetric profiles transverse to these crests, abrupt contacts with other units, and continuity in the vicinity of topographic obstacles such as impact craters indicate that they are not modern dunes but instead are an erosional expression, perhaps caused by exhumation of paleodunes or differential erosion along joints formed within the thin mesa unit (*21*). Some of these units may be shedding sand-sized particles that contribute to nearby dunes and drifts of similar albedo.

The physical characteristics of all three unit types suggest that they consist of indurated fine-grained material. Evidence for induration comes from the presence of steep cliffs and escarpments, even among thin mesa units (Figs. 1, 4, and 5), wind-sculpted ridges (yardangs), preservation of fault contacts and offsets (Fig. 6), and lack of blurring between adjacent beds of contrasting albedo (Figs. 4E, 5, and 6). Ad-

ditional evidence for induration comes from the observation that where windblown sand is present, it does not accumulate on outcrop surfaces [except in thin streamers or in the lee of small obstacles (Fig. 7A)], suggesting that the outcrop surfaces are hard and resistant to the impact of saltating grains. Evidence that the outcrops consist largely of fine grains [e.g., clay, silt, sand, and granule sizes (*22*)] comes first from a lack of boulders at the base of escarpments (*23*) formed in these materials (which indicates that when eroded, they break into clasts smaller than boulders) and second from the presence of yardangs [that form by grain release in materials which break down into fine grains and are transported away by eolian saltation and traction (*24*)]. In the vicinity of some outcrops, such as "White Rock" in Pollack Crater (Fig. 7B), light-toned material tops the crests of large eolian ripples, indicating that the outcrops break down into fine materials [most likely granules (*25*)].

The geometry of many of the outcrops suggests that the materials are horizontally bedded (Fig. 4), although some are locally dipping in conformance with crater wall slopes (*26*). Outcrops typically exhibit unambiguous stratigraphic relations such that one type of unit is clearly overlain or underlain by a unit or units of different properties and expression. In Terra Meridiani, such relations extend over hundreds of kilometers (Fig. 8).

Figure 9 offers a detailed example of the complexity of outcrop stratigraphy. It shows a geologic map (*27*) and cross section through a portion of a ~2.3 km high, 6000-km^2 mound that occupies about 50% of the floor of a 150-km-diameter impact crater, Gale. Eleven units, numbered according to inferred stratigraphic placement (oldest = 1), were identified by distinguishing the top and bottom (except for the two topographically lowest units) contacts between units of differing tone, texture, and other physical properties (*28*). A gap in the stratigraphic record—an unconformity representing a period of nondeposition—occurs at the top of unit 6, shown by the presence of partly exhumed impact craters at the top of the unit (Fig. 9C) and an exhumed channel that cuts into the unit (Fig. 9E). This example illustrates the enormous volumes of material transported to and deposited within such locales, the substantial amount of time needed to create such deposits, that they were subjected to a host of processes while forming, and that other equally powerful processes subsequently eroded and removed large percentages of these materials.

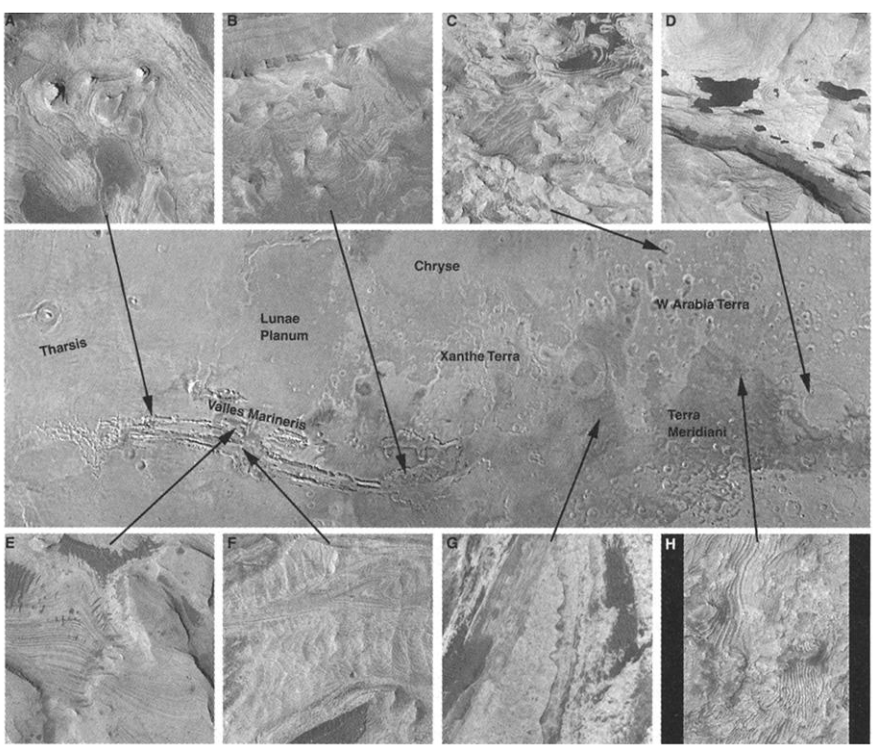

Fig. 1. Eight examples of very similar outcrops of light-toned, layered, cliff-forming material exposed in locations separated by hundreds to thousands of kilometers. This map extends ~9600 km across equatorial Mars (±25° latitude) from 120°W to 340°W. Examples are subframes of MOC images, each is illuminated from the left, shown at the same scale, and covers 1.5 km by 1.5 km. (**A**) Tithonium Chasma, 5.0°S, 89.7°W, M08-04701. (**B**) Capri Chasma, 13.1°S, 49.4°W, M11-00862. (**C**) Becquerel Crater, 21.7°N, 8.0°W, M02-02717. (**D**) Crater in northwest Schiaparelli Basin, 0.2°S, 345.5°W, M10-00798. (**E**) West Candor Chasma, 6.3°S, 75.9°W, M07-05599. (**F**) Melas Chasma, 8.8°S, 74.2°W, M09-02145. (**G**) Iani Chaos, 4.1°S, 18.5°W, M13-01484. (**H**) Crater in Terra Meridiani (black areas have no coverage), 2.8°N, 359.0°W, M08-00170.

Geologic and Geographic Settings

Most of the outcrops occur in groups between ±30° latitude (Fig. 2), although there are numerous examples at higher latitudes (*29*). There are four regional-scale occurrences: Valles Marineris, Mawrth Vallis and west Arabia Terra, Terra Meridiani, and northern Hellas. An additional but more spatially distributed group occurs in southern Elysium Planitia/Aeolis. With a few exceptions [e.g., banded material in Holden Crater (Fig. 4E)], unit types and the general aspects of the vertical sequence are repeated in different locations and geologic settings, even in cases separated by hundreds or thousands of kilometers (Fig. 1). For example, where they occur together, massive units are always above layered units, and dark-toned, thin mesa units always overlie lighter-toned layered and massive units.

The outcrops occur in four different geomorphic settings: crater interiors, intercrater terrain (*30*), chaotic terrain, and chasm interiors. Many of the craters in which layered outcrops occur are in western Arabia Terra (Figs. 4A and 7A). Others are scattered across equatorial Mars and include Holden Crater (Fig. 4E), Gale Crater (Fig. 9), and craters in western Terra Tyrrhena. Outcrops in craters are usually expressed in one of two forms, either in the floors and walls of pits that have developed within materials that mostly or partially fill the crater, as with Terby (Fig. 4C), or as mounds and mesas that stand higher than the present crater floor, as with Gale (Fig. 9). In some cases, both pits and mounds are present. Outliers of the light-toned material can often be found many kilometers from the main outcrop body, both on the floor of the crater and on the interior crater wall; this is the case, for example, in Trouvelot Crater (Fig. 10) (*31*). Such relations suggest that each mound or mesa is a remnant of a formerly more extensive unit or group of units within the crater; for example, the mound in Gale (Fig. 9) must at one time have extended across and throughout the entire basin, perhaps filling it to its rim. Figure 11 illustrates a possible sequence in the stages of erosion and exposure of layered outcrop materials seen in large (~150 ± 75 km diameter) impact craters, progressing from those that are nearly completely filled (Fig. 11A), to those that have developed pits around the circumference at the interface between crater wall and filling material (Fig. 11B), to those in which the outcrop material is entirely isolated from the walls but still nearly fills the crater (Fig. 11C), to those of progressively smaller interior mounds and mesas (Fig. 11, D and E).

Outside of impact craters, the most areally extensive exposures of layered units occur in the intercrater plains of northern Terra Meridiani (Figs. 2 and 8). The Terra Meridiani units embay and bury impact craters, and some of these craters are in various states of exhumation (e.g., Fig. 4D). An extensive (~200,000 km^2),

intermediate- to dark-toned thin mesa unit, mostly expressed as ridged-and-grooved terrain that unconformably overlies light-toned layered units (*32*), corresponds to the surface detected by the MGS Thermal Emission Spectrometer (TES) as being enriched in hematite (*33*). Other intercrater terrain examples include light-toned material resembling the Terra Meridiani units exposed from beneath a smooth-surfaced, dark mesa unit at the distal end of Mawrth Vallis in west Arabia Terra (*34*), yardang-forming layered units in the Aeolis region (*35*), and light- and dark-toned layers exposed in pits among the massifs of the northern rim of the Hellas Basin (*36*). The units among craters and massifs of north Hellas resemble and are probably similar to those in Terby Crater (Fig. 4C). Regional slope (toward the northwest) and the presence of broad, cliff-bounded shelves interpreted to be mantled layered outcrop throughout intercrater terrain in western Arabia Terra suggest that the units at Mawrth Vallis are exhumed from beneath strata deeper in the martian crust than those seen in Terra Meridiani.

Westward from Terra Meridiani, in northern Margaritifer Terra, outcrops of light-toned massive and layered material are found in chaotic terrain (*37*). These regions consist of heavily cratered terrain that has been disrupted and broken into hundreds of small buttes and mesas, some of which correspond to the location of filled, partly buried, or formerly buried impact craters, and some of which connect directly to large outflow channels (particularly, Ares Vallis). The largest exposures of layered material in chaotic terrain occur in Aram Chaos (*38*); others, as in Fig. 1G, are in circular or somewhat circular depressions such as Iani Chaos (*39*). Despite the difference in geomorphic setting, these appear to be units that mark the sites of old, filled, and buried impact craters similar to those in western Arabia Terra that were subsequently disrupted by the chaos-forming processes.

From the chaotic terrain of Margaritifer Terra, the Valles Marineris consists of a series of troughs, chasms, and pit chains that stretches more than 3000 km westward to Tharsis. MOC images show the outcrops seen in Mariner 9 and Viking images of the Valles Marineris chasms in much greater detail; more important, they reveal many occurrences that were not previously identified. The most extensive and morphologically diverse exposures are in western Candor Chasma (Figs. 3, 4B, and 5). The fewest exposures are in areas where no pre-MGS examples were identified (e.g., Noctis Labyrinthus). Relative to west Candor, other chasms exhibit greater amounts of surficial cover by dark- or intermediate-toned materials, landslide deposits, and other debris that are in contact with, and therefore inferred to obscure, additional occurrences of the layered and massive material. Contact relations between chasm wall rock and the interior light- and intermediate-toned outcrops are in most places difficult to see because the walls and floors are largely covered by a dark-toned mantle that either is or superficially resembles thin mesa unit material. However, a few MOC images reveal important contact relations: several MOC images [Fig. 12 and (*40*)] show outcrops of light-toned layered units sticking out of the chasm walls and three images of layered units at the contact between chasm floor and wall in northwestern Candor Chasma show the layered units to continue into and under the walls (*41*).

Interpretations

Nature of outcrop materials. The layered, massive, and thin mesa units are interpreted to be outcrops of martian sedimentary rock. They are rock because they are indurated (*42*). The outcrops have the attributes of material emplaced as sediment because they exhibit evidence of being fine-grained and bedded. Among layered units, the widespread occurrence and repetitious nature of many of the outcrops (Fig. 4, A and B) are especially suggestive of sedimentary origin (*43*).

Age relations. Impact craters are traditionally used to estimate the relative and absolute ages of planetary landforms; older surfaces have more craters within a given diameter range per unit area than younger surfaces. The age of the layered, massive, and thin mesa units cannot be easily determined by this traditional means because they have very few impact craters on them. Where impact craters do occur, they are in some cases seen to be interbedded with the layered units or partly exhumed from beneath these units (Figs. 4D and 9C). Exhumation of craters and cratered surfaces compromises the utility of impact crater counting to determine age. The absence of impact craters on most outcrop materials suggests that the surface exposures are too young to have had craters formed upon them (*44*). Assigning an absolute age to surfaces at the scale of MOC images that have few or no craters (and the added complication of possible exhumed craters) is impossible (*45*).

The age of the outcrop materials can only be determined approximately by examining their geologic context and stratigraphic placement. Here we focus on the layered and massive

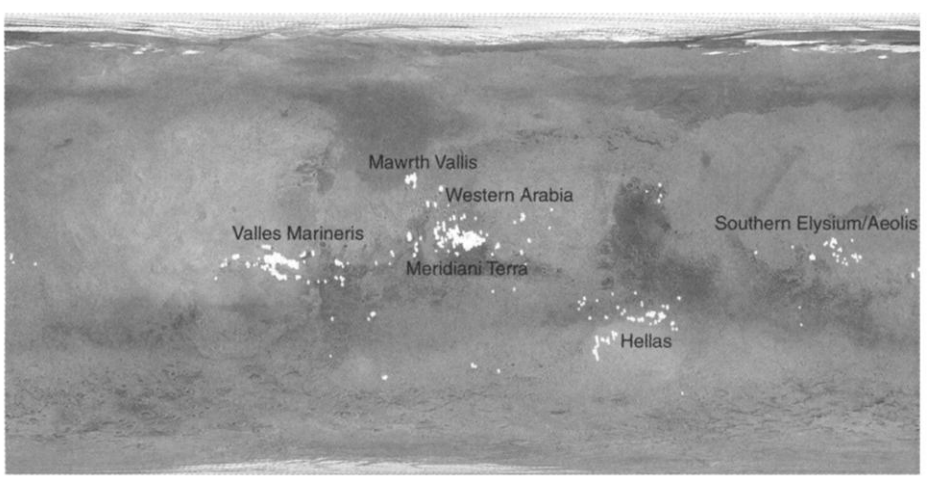

Fig. 2. Simple cylindrical equal angular map of Mars (centered on 0° latitude, 0° longitude) showing locations of all light, intermediate, and dark-toned layered, massive, and thin mesa unit outcrops in MOC images obtained through 31 October 2000.

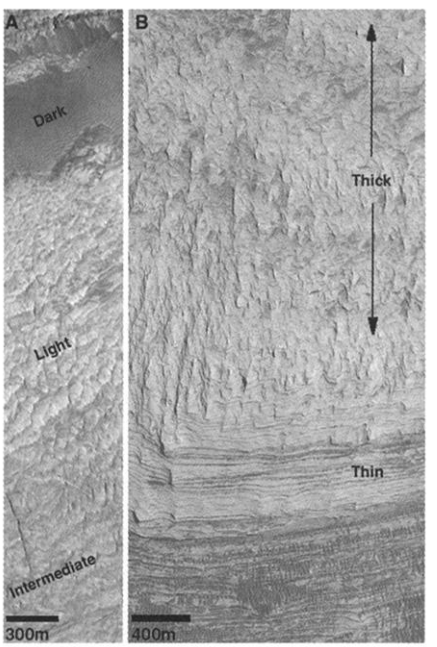

Fig. 3. (**A**) Illustration of the relative brightness of light-, intermediate-, and dark-toned outcrops (subframe of MOC image M09-06480 in west Candor Chasma near 6.1°S, 76.1°W; illuminated from the upper left, north is up). (**B**) Illustration of the relative thickness of thin- versus thick-bedded outcrops. The surface slopes downward to the bottom of the frame. Thin beds are generally thinner than 200 m, thick units can be in excess of 1 km. The thick material also illustrates a typical massive unit (subframe of M10-02361 near 5.7°S, 73.2°W, on Candor Mensa, illuminated from the right, north is toward lower left).

units; thin mesa units lie unconformably on top of eroded exposures of layered and massive units, and thus represent deposition that occurred some time later than the deposition, diagenesis, and erosion of the layered and massive units. Two sets of observations are relevant to establishing the age of the units: their position relative to the sequence of materials seen within the Valles Marineris and their relation to large impact craters. The occurrence of light-toned layered outcrops within and coming out from under the walls of the Valles Marineris (Fig. 12) has profound implications. The plains into which the chasms are cut have been dated as Hesperian in age (*46*, *47*), and discussions of previously observed layers in the walls of the Valles Marineris concluded that the wall material must be no younger than the Early Hesperian, with the bulk of material being Noachian (*48*). Four additional observations permit this age to be applied to other locales: (i) Wherever they occur, these units display similar material properties, geomorphic expressions, and stratigraphic relations (Fig. 1). (ii) Occurrences in craters—from completely filled to isolated buttes—are pervasive. (iii) Outcrops in chaotic terrain mark either the locations of obvious, filled impact craters (e.g., Aram Chaos) or circular depressions that appear to have once been impact craters (e.g., Iani Chaos). (iv) Many of the Valles Marineris troughs have circular or semi-circular indentations (e.g., south Melas Chasma wall) and termini (e.g., west wall of west Candor Chasma), suggestive of structural control by buried craters. These observations indicate that the outcrops of light- and intermediate-toned layered and massive materials in the Valles Marineris and adjacent chaotic terrains are either very similar to or the same types of materials that are found in the craters of western Arabia Terra and elsewhere. Outcrops in the Valles Marineris and adjacent chaotic terrains appear to represent the locations of impact craters that were filled with layered and massive material, then subsequently buried by the materials that form the Lunae, Syria, and Sinai plains. Later faulting and landsliding are responsible for present visibility (*49*). Thus, the outcrops of layers found on the floors of the Valles Marineris are old (Noachian), and by virtue of their many similarities, we suspect that those found in large craters elsewhere on Mars are equally ancient.

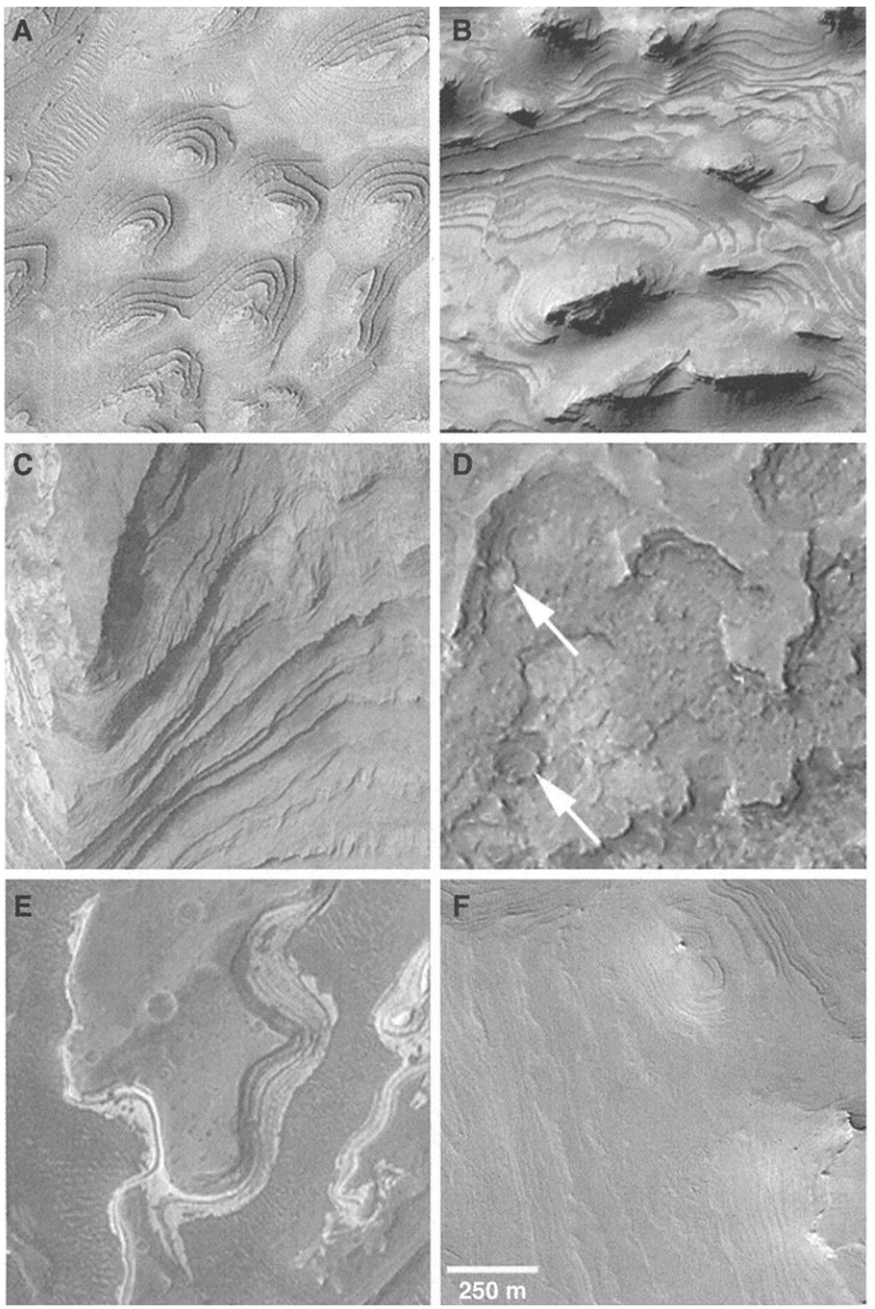

Fig. 4. Examples of layered unit outcrop expressions. (**A**) Stair-stepped hills in an impact crater in west Arabia Terra near 8.3°N, 7.1°W. (**B**) Cliff-bench terrain in southwestern Candor Chasma near 6.4°S, 77.1°W. (**C**) Irregular cliff-bench on slope in Terby Crater near 27.6°S, 285.7°W. (**D**) Cliff-bench terrain in which different layers have differing tone and are interbedded with small exhumed and partly exhumed impact craters (arrows) at Terra Meridiani near 5.0°N, 2.5°W. (**E**) Alternating light- and dark-toned, banded outcrops in Holden Crater near 26.9°S, 34.9°W. (**F**) Dust-mantled (uniform tone) cliff-bench outcrops in Henry Crater near 11.1°N, 335.5°W. Shown at the same scale, each picture is a subframe of a MOC image illuminated from the left. (A) M09-01840, (B) FHA-01278, (C) M04-03686, (D) M03-01935, (E) M08-02225, and (F) M12-02473.

Origin of layered and massive unit material. The geographic distribution, physical attributes, and Noachian age of the layered and massive units imply that the processes by which the materials were deposited are no longer those that occur on Mars today, at least with the same vigor. The scale of the observed outcrops argues for processes that operated over great distances and involved enormous volumes of material [for example, the 165-km-diameter crater, Henry, located at 11.0°N, 336.8°W in Arabia Terra, contains ~10,000 km^3 of layered units in a single mesa (Figs. 4F and 11C)]. Despite the large volumes of material involved, no source regions for the sediments are obvious at the surface of Mars today, nor are the transportation paths that brought the materials to the locations in which they are found. For Henry Crater to have been filled to or nearly to its rim, the surface across which transport of sediment occurred might well have been topographically higher than the present crater rim, a relation not seen today. This surface, and perhaps some fraction of the relief on the original crater rim, have been eroded subsequent to the emplacement of the sediment such that little, if any, trace of them remains today.

Processes most likely to have been major contributors would have to be those that can create kilometers-thick deposits that can fill

impact craters over 100 km in diameter (Fig. 11). These processes could not be isolated or local, as they have affected large portions of the planet by creating similar deposits separated by hundreds and thousands of kilometers. As a further constraint, the processes had to create in Terra Meridiani layered units of similar thickness, physical properties, and great areal extent that are not confined within a specific crater or chasm. The MOC images showing the scale and extent of outcrops in Terra Meridiani (Fig. 8) are reminiscent of aerial photographs of the sedimentary rocks of the Colorado Plateau in Arizona and Utah, which formed over half a billion years in environments that changed over time and included a variety of subaqueous and subaerial settings. By analogy, and for the moment refraining from speculation about unknown martian processes with no terrestrial counterpart, the martian outcrop materials are most likely to have been deposited under subaerial and/or subaqueous conditions (*50*).

Subaerial transport and deposition of sediment occurs on Mars today (e.g., dust storms, dust mantles, and sand dunes) and, thus, must also have occurred in the past. Volcanic, impact, and eolian processes could individually and jointly have contributed material subaerially to the layered, massive, and thin mesa units. From terrestrial experience, it is known that volcanism can produce pyroclastic deposits that drape older terrain by air fall, can include kilometers-thick massive units, and can occasionally display thick sequences of repeated beds [such as those formed in pyroclastic surge eruptions (*51*)]. However, pyroclastic units of thickness in excess of a few centimeters are rare except within hundreds of meters to a few tens of kilometers of their source vent (depending on magnitude of individual eruptions); distal deposits—airfall—thin radially outward from vents and are usually measured at scales of millimeters and centimeters. If explosive volcanism were responsible for the outcrop materials, their presence would require that Mars has produced eruptions with cumulative volumes in excess of those found on Earth while retaining no evidence of the volcanic vents from which the materials came; the vast majority of the locations of layered and massive outcrops are quite remote from manifestations of volcanism. Explosive volcanic eruptions of this type on Earth occur because of substantial changes in magma composition resulting from processes of crustal formation and evolution attending plate tectonics. If the observed materials are pyroclastic, they would define an early Mars whose geophysics was very different from the planet today, and for which other forms of geologic evidence are not seen.

As with volcanism, sedimentation by impact crater ejecta emplacement is localized near the source. In this case, most material that actually comes out of the impact-produced cavity falls within one crater radius of the rim. In terms of volcanism and impact cratering, only deposition of small clasts (silt and clay particle sizes) produced by these events and then transported in suspension by the atmosphere might contribute to layered, massive, and thin mesa units; however, the great areal extent (Fig. 2) and volumes of material involved (the volume cited above for Henry is but one small example) would require that these materials are produced in truly prodigious quantities.

Atmospheric transport of fine debris is the one subaerial process capable of having made major contributions to the martian outcrop units. Cross beds would be good indicators of eolian transport via saltation and traction, but no cross bedding is observed in MOC images. This could indicate that none of the outcrop materials were deposited as eolian sands, but it

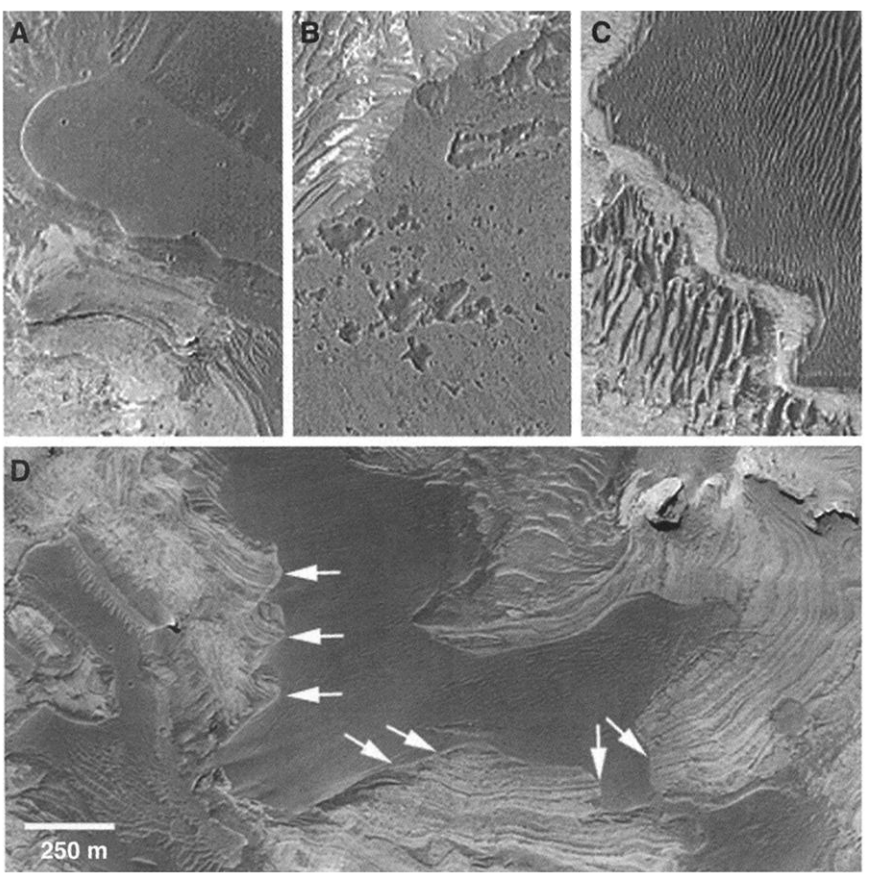

Fig. 5. Examples of thin mesa unit outcrop expressions. (**A**) Typical, dark-toned, smooth-surfaced thin mesa unit located in west Candor Chasma near 7.3°S, 74.8°W. (**B**) Pitted thin mesa unit in west Candor near 6.9°S, 74.8°W. (**C**) Ridged-and-grooved, dark-toned, thin mesa unit (note the sharp edge along the southern and western boundary that runs approximately from upper left to lower right) located in west Candor near 6.9°S, 74.6°W. (**D**) The dark mesa unit on which arrows are drawn occurs on a hill; arrows indicate locations where the mesa unit cuts across and covers layers of the underlying unit. This example of an erosional unconformity is located in west Tithonium Chasma near 5.0°S, 89.7°W. Shown at the same scale, each picture is a subframe of a MOC image illuminated from the left/upper left. (A and B) M03-01870, (C) M02-01705, and (D) M08-04701.

Fig. 6. Layered outcrops offset by faults (unlabeled arrow indicates one example). Preservation of faults and lack of albedo "smear" between beds indicates that the layered material is firm and immobile. Subframe of MOC image M00-01882 in west Candor Chasma near 6.8°S, 75.5°W, illuminated from the upper left.

is likely that cross beds would be too small to be seen in these typically 1.5- to 6.0-m/pixel pictures. Deposition from suspension would explain the lack of obvious transport pathways on the martian surface, and it would allow incorporation of fine clasts generated by volcanism, impact cratering, as well as weathering and erosion. Whether processes exist that could produce the enormous volumes of material observed, and whether deposition from suspension could create regular, repeated beds as seen in some layered units (Fig. 4), is unknown.

Subaqueous depositional processes include those associated with flowing water (alluvial), standing water (submarine and lacustrine), and the mixing of flowing water and standing water (deltaic). Despite the absence of well-defined overland transport systems of gullies, channels, streams, and valleys, alluvial processes may have played a major role in the formation of the martian outcrop materials. The valley networks found in the cratered hemisphere on Mars (*52*, *53*) might represent the heavily mantled, mostly eroded, and/or exhumed remnants of that transport system (*54*, *55*). However, valley networks are notably absent from the areas where the sedimentary rocks are found. Had valley networks been the conduits of material, they are now either buried so deeply that no surface manifestation is apparent or they occurred in a layer destroyed by subsequent erosion. In either case, the absence of evidence makes it difficult to ascribe any relative importance to their contribution. Likewise, there is no evidence, either from location within a depositional basin (for example, a mound of layered or massive material at the mouth of a gully) or from high-resolution observations of stratigraphic relations (such as foreset bedding), that deltaic processes contributed to the martian landforms.

Subaqueous environments include both deep and shallow water locations. Notwithstanding locations for biogenic and evaporitic precipitation, deep water locations are generally those wherein relatively thick, undifferentiated layers accumulate over long periods of time in quiescent environments. Shallow water locations are those wherein relatively thin layers with a high degree of variability in the caliber and composition of constituents occur, accumulating over short periods of time in energetic or turbulent conditions. Evaporites develop in "shallowing" water (or at least in water in which evaporation is changing the volumetric relations of water to solutes). Marine and lacustrine environments are distinguished, in this context, primarily by the areal and volumetric extent of the body of water.

The affinity of the layered materials for impact craters, including those subsequently buried and then exposed in the walls and interiors of the Valles Marineris and adjacent chaotic terrain, suggests that lacustrine processes may have contributed to the formation of the layered units. Observations that support this view include the thicknesses of crater-filling deposits, their position within and around the craters (especially their dip with respect to crater wall topography), the occurrence of chaotic terrain and its relation to in-filled craters, and the number of cases in which crater-filling units are regularly layered. The latter evidence argues for relatively shallow and energetic, episodic periods of deposition, more likely to occur within smaller, closed depressions than in larger basins.

The broad surface expression of the layered materials in Terra Meridiani and similar occurrences (e.g., in the northeastern Hellas rim region and Mawrth Vallis) constitute important exceptions to the preference of such materials to closed basin environments. These units embay, fill, and cover craters and other pre-existing landforms almost without regard for their relief, but do so with relatively thin deposits. In the case of northeastern Hellas, these units might be an extension of unseen layers beneath the rugged, mantled surface of the Hellas Basin floor. Parts of the northwestern Hellas Basin floor do, in fact, exhibit layered outcrops (Fig. 2), and it might be argued that Hellas was the site of a basin-wide sea. The Mawrth Vallis and Terra Meridiani cases are more problematic. Their deposition patterns may indicate that, at

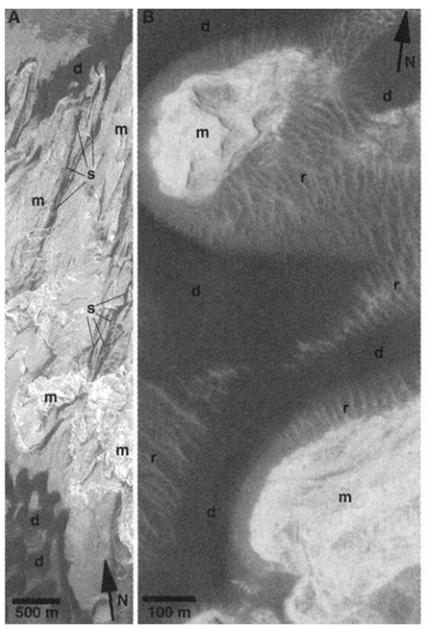

Fig. 7. (**A**) Dark, windblown sand dunes (d) on either side of light-toned, layered mounds (m) in Becquerel Crater near 21.5°N, 8.5°W. Only thin streamers of sand (s) occur on the mound, indicating that the light-toned material is hard. Subframe of MOC image M07-01459, illuminated from the left. (**B**) Large, windblown ripples (r) with light-toned crests associated with low-albedo sand (d) and light-toned, cliff-forming, layered material (m) in Pollack Crater near 8.1°S, 335.1°W. Light-toned material at the ripple crests is inferred to have been derived from the erosion of the nearby light-toned outcrops, suggesting that the outcrops weather and erode into particles of sand or granules. Subframe of MOC image M13-00459, illuminated from the upper left.

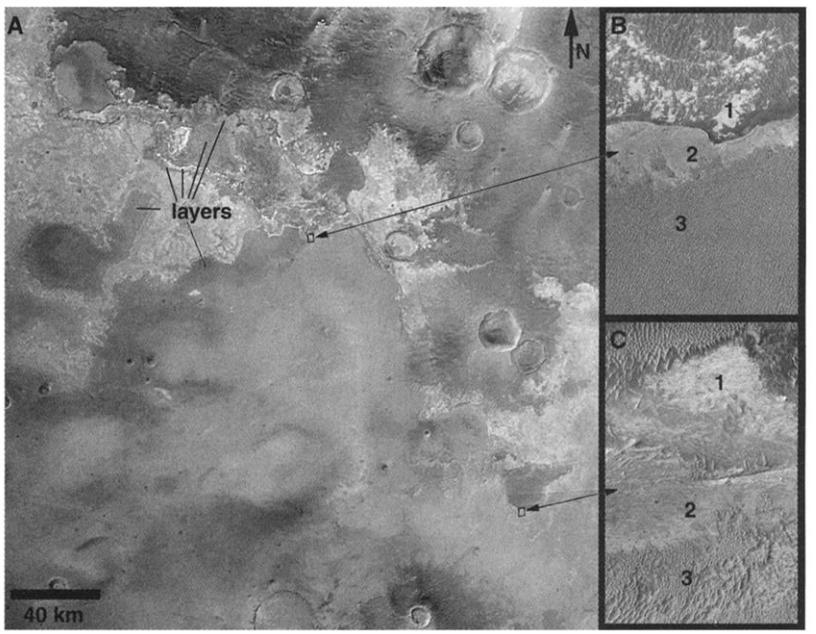

Fig. 8. Example of lateral continuity of stratigraphic units over distances >100 km in northern Terra Meridiani. (**A**) Colorado Plateau–scale outcrops of light-, intermediate-, and dark-toned strata ("layers") in planimetric view in a regional image. Small boxes indicate locations of two MOC narrow-angle image subframes, (**B**) M02-04582, and (**C**) M00-02426. Numbers 1, 2, and 3 indicate in stratigraphic order (1 is oldest) strata of the same tone, texture, and outcrop expression in each of the two high-resolution views. Regional view is from a mosaic of MOC red wide-angle images M01-01236, M01-01238, M01-01627, and M01-01629. All pictures are illuminated from the left; the center of the regional view is near 0.5°N, longitude 0°.

the time that the region's craters had lakes in them, the surrounding intercrater plains were also submerged and were the site of shallow marine deposition.

The absence of any corroborating evidence for lacustrine or marine processes is obviously a substantial weakness of this idea. There are, for example, no residual high-standing sources of primary or recycled rock materials that might have been the source of materials filling, for example, the intercrater plain of northern Terra Meridiani, or northeastern Hellas. As with the case of alluvial processes, there is no evidence of a transportation network leading to these sites. Bodies of water have an additional mechanism by which they can create deposits: precipitation. An alternative view would posit that much of the layered material is not clastic but formed by precipitation of salts, including carbonates derived from atmospheric CO_2. However, the lack of strong, obvious carbonate or evaporite mineral signatures in infrared spectra of Mars (*56*, *57*) indicates that either their signature is masked from orbiting spectrometers (e.g., by silicate dust and/or the carbon dioxide and water ice/vapor of the atmosphere), or these minerals are present, at most, as minor constituents.

Age and origin of thin mesa units. Most of the dark and intermediate-toned thin mesa units are not Noachian; they formed much later. Their relative age is indicated by the fact that the they lie unconformably on layered and massive unit surfaces that were already eroded to approximately their present topography. The superposition of dark mesa-forming material on slopes within the Valles Marineris, both on chasm walls and walls of mesas such as Candor Mensa, indicates that this material was emplaced after the chasms formed. Oddly, they are often substantially more cratered than the subjacent layered or massive units.

The nature, origin, and processes that govern the distribution of thin mesa unit materials are unknown. The ridged-and-grooved erosional form some units take may be the expression of paleodunes, which would indicate sand-sized particles and a genesis by eolian sedimentation, but the manner in which they drape over pre-existing topography is more consistent with airfall deposition than saltation. The draping nature of the thin mesa materials and their occurrence in nearly all regions where layered and massive units have been exposed are most suggestive of wide distribution and deposition from suspension in the martian atmosphere.

Exposure of material. Not only is evidence of the depositional processes not apparent, neither, in most cases, are the processes that ex-

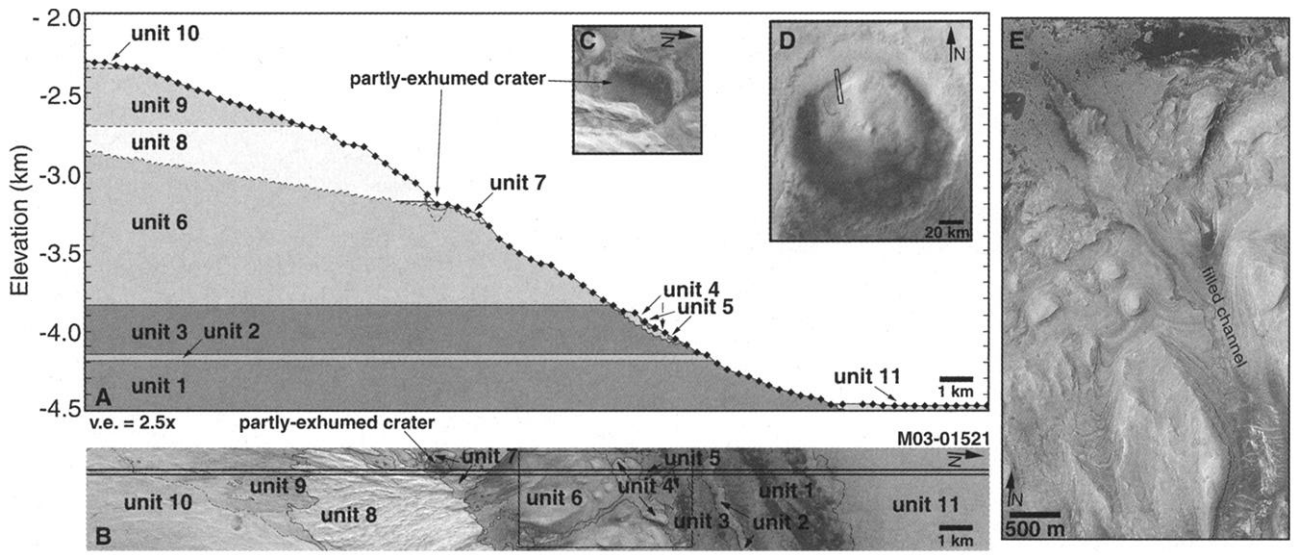

Fig. 9. Gale Crater (5.4°S, 222.2°W) central mound stratigraphy based on MOC image M03-01521 and the simultaneously acquired topographic profile. (**A**) Geologic cross section through northern portion of ~2.3-km-high mound. Black diamonds indicate location, approximate size, and uncertainty of individual laser altimeter shots used to derive topographic profile; elevations are relative to the martian datum. Geologic units (*28*) are interpreted to lie horizontal—except where erosional unconformities have been identified—because the plain immediately north of the mound (unit 11) is horizontal. (**B**) Geologic map; units numbered according to stratigraphic placement (1 is oldest). Box near center indicates location of area illustrated in (**E**). (**C**) Close-up of partly exhumed impact crater formed in upper surface of unit 6 marking location of an unconformity. (**D**) Gale Crater; box shows location of image M03-01521. This is a cropped mosaic of MOC red wide-angle images M01-00352 and M01-00740. (**E**) Detailed view of unit 6 layered outcrops and filled channel cut into the unit, indicating location of erosional unconformity.

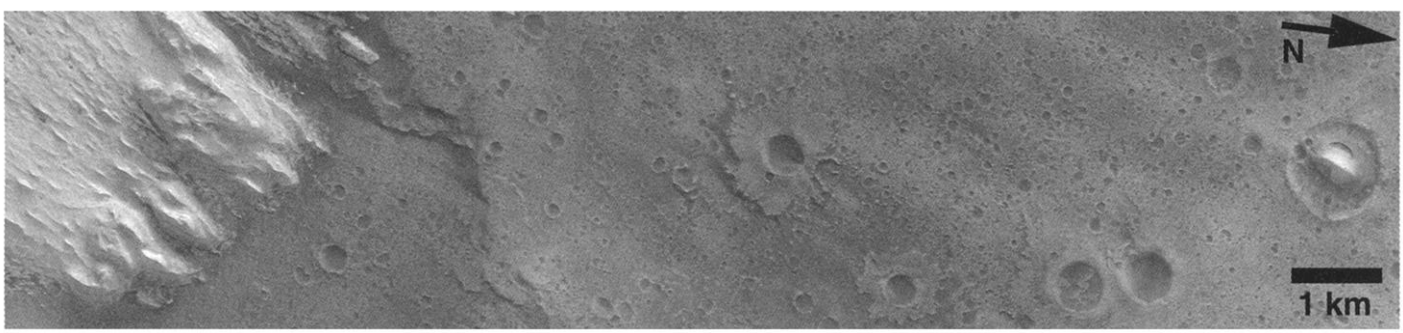

Fig. 10. Remnants of a more extensive layered unit that may have covered the entire floor of Trouvelot Crater (15.5°N, 12.3°W). At left is a small portion of a 7.5 km by 18 km light-toned, ridged-and-grooved mound in south-central Trouvelot. At right is a small outlier of the light-toned material located ~10.5 km from the main outcrop. Light-toned outliers also occur elsewhere in Trouvelot, including its southern wall (*31*). Subframe of MOC image SP2-53203, illuminated from the top/upper right.

posed and eroded the layered and massive units (with the obvious exceptions of faulting in the Valles Marineris and the presence of yardangs that imply wind erosion). For example, Henry Crater contains 10,000 km^3 of material in an isolated mound within the crater. This material is layered and stands nearly as high as the crater rim (*58*). This observation implies that some process or processes have removed 15,000 km^3 of material from Henry Crater. Notwithstanding recognition of morphologies that suggest an apparent sequence illustrating removal of material from impact craters (Fig. 11), the actual processes are unknown. The implication is that most of the exposure and erosion of the layered units must have occurred some time far in the martian past, when transport out of the craters (again, with no obvious transport pathways) could have occurred via processes not acting on the planet today. However, the absence of small, fresh-impact craters on the surfaces of these units indicates that some degree of erosion of the units is ongoing. Their continued existence argues that they have spent most of martian history hidden and protected from small impacts by thick eolian mantles or, perhaps more likely, by the thin mesa-forming units observed in nearly all outcrop localities.

Implications for early Mars. Early spacecraft pictures of Mars showed a cratered landscape different from the moon. The primary morphology of the largest impact craters (>20 km in diameter) was seen to be shallower than their lunar counterparts, with more subdued rims, flatter floors, statistically few central peaks, little evidence of ejecta blankets, and few, if any, secondary craters and/or rays (*59*). These observations were interpreted to indicate that the chief difference between Mars and the moon—the presence of an atmosphere—was responsible for having eroded the craters and filled their floors with the products of this erosion (*60–63*). Mariner 9 pictures presented new observations of martian erosional landforms, including the discovery of networks of small valleys throughout the heavily cratered terrain; these networks appeared to be old and were taken by many to be indicators that early Mars had been warmer and wetter than at present. It then seemed possible that craters in the Noachian terrains were not only degraded by wind, but also by running water. Crater studies that followed Mariner 9 suggested that a period of enhanced erosion occurred either while the majority of craters were still forming (*64*, *65*) or in an "obliteration event" or events after most of the craters were formed (*66*, *67*). In either case, the cratered terrains of Mars were seen to be a place somewhat like the moon—with its brecciated crust of impact-fractured material to depths of several kilometers—and with all of the crater degradation explained by imposition of erosion (valley networks, outflow channels, wind scour) and deposition (of sediments locally derived from erosion of crater walls, rims, and central peaks and of lava flows in volcanic regions) (*68*, *69*). This is the view of Mars that pervades contemporary studies.

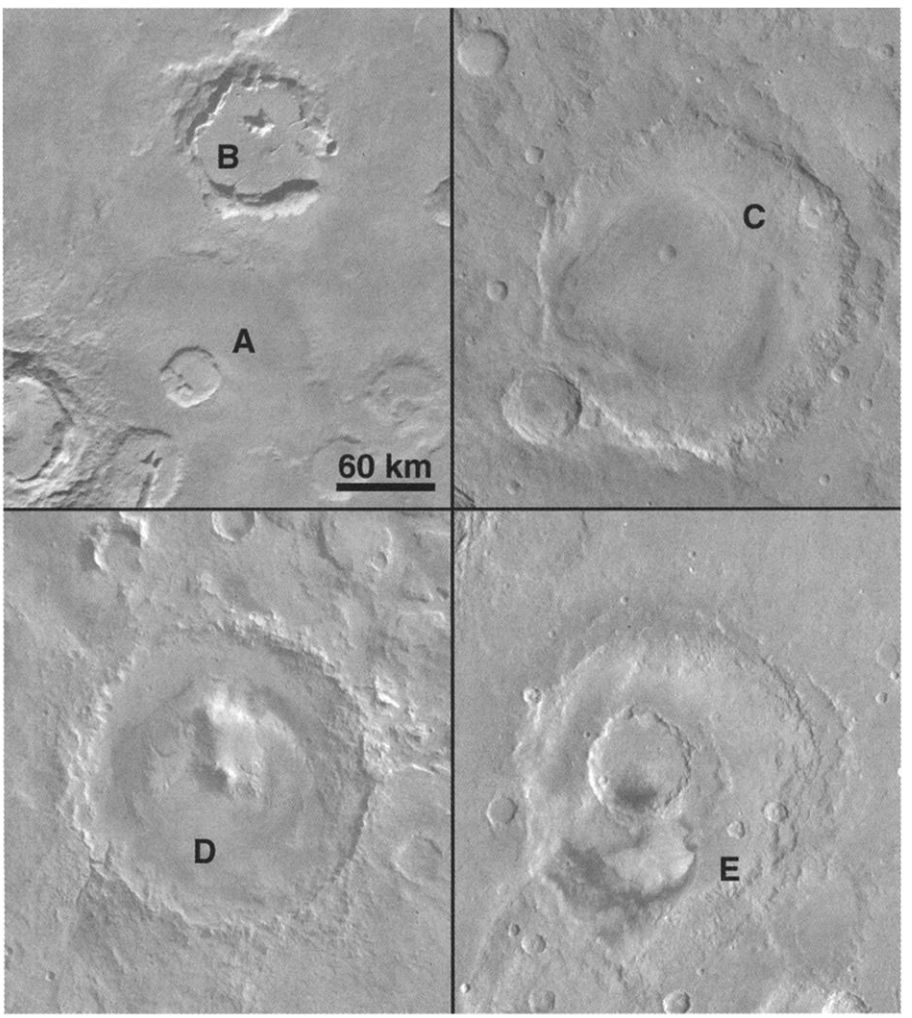

Fig. 11. Illustration of a possible sequence (**A** through **E**) for the removal of layered material that has filled impact craters of ~150 ± 75 km in diameter. Images are subsections of U.S. Geological Survey Viking orbiter image mosaics, shown at the same scale. With the exception of the crater at (A), the materials filling all examples are known to include layered units; a few also have massive units. (A) Filled, unnamed crater, 49°S, 355°W. (B) Initial removal occurs at the interface between the crater wall and the fill material, unnamed crater, 47°S, 355°W. (C) Large isolated mesa of layered material at crater center, Henry Crater, 11°N, 336°W. (D) Layered fill reduced to a mound that stands nearly as high as crater rims in Gale Crater, 5°S, 222°W. (E) Relatively small, isolated mound containing layered outcrop material, Becquerel Crater, 22°N, 8°W.

Hints within Mariner 9 images suggested that this view was not complete. Observations suggested apparent burial and exhumation relations for a small number of craters (in some cases involving as much as a kilometer of overburden), and topographic measurements indicated that layered materials within the Valles Marineris occupied a substantial fraction of the vertical relief within the chasms. Such information led to the proposal that layering occurred planet-wide and that it resulted from materials emplaced by impact ejection, eolian, volcanic, and fluvial processes, simultaneously with the formation of craters (*70*).

From the earliest MOC images, observations strongly indicated that the upper crust, to depths as much as 10 km in the deepest parts of the Valles Marineris, were not brecciated but instead layered (*48*, *71*). Subsequent thousands of MOC images have shown that nearly everywhere the subsurface of Mars is exposed—in the walls of impact craters, troughs, and channels—the crust or bedrock of heavily cratered Noachian terrains is layered (*72*). The new observations presented here focus on a specific suite of layered materials that present a Mars in which impact cratering and the processes that formed layers were happening at the same time, a Mars in which craters and Noachian cratered terrain have not only experienced erosion, but enormous amounts of exhumation to expose materials deposited during that time.

We consider two possible scenarios for early Mars. The first, and perhaps favored, model draws heavily on comparison to Earth to invoke

a planet and environment capable of sustaining liquid water on its surface, and the movement by this water of substantial amounts of eroded rock material. The many occurrences of layered sedimentary rock units in craters or crater-like depressions argue for small, closed depressions acting as catchment and depositional basins; the few locales of regional layering without obvious basin control argue further for the possible existence of shallow seas. No evidence yet requires invocation of global oceans. Repetitious layering and changes in layer thickness indicate that this Mars experienced dramatic variations in surface conditions. The timescales, magnitude, and nature of these variations are not known today.

Fig. 12. Example of light-toned layered units exposed in the wall of the Valles Marineris. A ridge (or spur) that runs down the wall [slope is toward the bottom in (B)] is mantled by dark, smooth-surfaced material, but small windows (arrows) through the mantle show that the spur, too, consists of light-toned material. (**A**) Context in northeastern west Candor Chasma (subframe of MOC image M17-00468 with 3-km-wide box indicating location of the high-resolution view). (**B**) Subframe of M17-00467. Both pictures are illuminated from the upper left and located near 5.2°S, 74.3°W.

This model of Mars is likely to appeal to the Mars astrobiological community, which has long expressed an interest in finding on the planet's surface evidence of materials of lacustrine origin formed early in martian history (*11*). Until now, it has not been certain that such materials actually exist on Mars. The pictures described here, in fact, show exactly the types of materials in which the record of martian life, if it ever existed, is most likely to be preserved.

The second scenario is substantially more exotic and attempts to conceive a plausible but uniquely martian explanation for what is observed. In this model, modulation of atmospheric pressure by astronomical perturbations, combined with catastrophic modulation of sediment sources, gives rise to conditions recorded by the layered, massive, and thin mesa units. It is thought from theoretical models that the present atmospheric pressure on Mars is buffered by carbon dioxide on the surface (*73*) or within surficial materials (*74*). Astronomical perturbations are likely to lead to variations in pressure of two orders of magnitude (0.1 mbar to 10 mbar) on timescales of tens of thousands to hundreds of thousands of years (*75–78*). If such influences can be extended to a period when the martian atmosphere was denser, it is possible that the martian environment might have been able to periodically suspend and transport substantially more material at some times and not others. Exactly what the conditions would be like on a planet in which 100-km-diameter craters were regularly formed on timescales shorter than hundreds of thousands of years is unclear, but certainly the ability of the ejected material to reach distant locations and create beds of nearly uniform thickness would vary greatly with atmospheric pressure. The same would be true for fragmental products of volcanic eruptions. In this scenario, atmospheric processes of erosion and deposition take center stage, with fluvial processes responsible for formation of valley networks and weathering processes working to modify distribution and expression of the voluminous and pervasive eolian units. Such a model might explain the apparent correlation between the end of heavy impact bombardment and the cessation of the most aggressive and dynamic agents of geomorphic change. It might even offer an explanation for the relation between the layered, massive, and thin mesa units: layered units formed during a time when the atmospheric pressure and impact flux rate were high, and layers record the punctuation of the steady formation of craters by large atmospheric pressure cycles. Later, when both the cratering flux and mean atmospheric pressure had declined, fewer craters and lower transport capacity might form layers much thinner than could be seen in MOC images; such deposits might appear massive. Lastly, as the cratering flux and mean atmospheric pressure fell to contemporary values, tens of millions to hundreds of millions of years might be needed to accumulate even the relatively thin beds of the mesa-forming units.

Of course, these two scenarios are not mutually exclusive, and a combination of the two obviously explains more than either individually. When applied to the two questions posed at the outset of this research article, our results show no evidence for climate excursions in the Amazonian but do provide evidence that can be used to support the contention that Mars in the Noachian was warm enough to be wet enough to sustain bodies of liquid water on its surface. But they can also be used to argue that Mars was very different from any of our previous views.

References and Notes

1. MGS was launched in November 1996 and achieved orbit about Mars in September 1997. Pictures taken through September 1998 were obtained from an elliptical orbit. The MOC was turned off from September 1998 to February 1999; it returned to service for the Primary or Mapping Mission in a 2 a.m.–2 p.m. equator-crossing, 370 km altitude, circular, polar orbit in March 1999. The Primary Mission is scheduled to continue through February 2001, with an extension at least through April 2002. The MOC (*79*) consists of three cameras: a narrow angle system that obtains high–spatial resolution images (1.5 to 12 m/pixel) and red and blue wide-angle cameras to acquire regional and global views (0.24 to 7.5 km/pixel).
2. Early Mars refers to the first 600 to 1000 million years after the planet formed, and corresponds to the time of intense impact cratering in the solar system and the emergence of life on Earth. Martian geochronology is divided into three periods: Noachian, the earliest, is defined as a period dominated by heavy impact cratering and widespread degradation of the cratered terrains; Hesperian, generally thought to be a short transitional time as the impact rate and other geomorphic processes acting to modify the heavily cratered terrain tapered off and major ridged plains units formed to cover considerable tracts of cratered terrain in places like Lunae Planum; and Amazonian, the recent period that includes Mars as it is seen today, in which the last volcanism occurred in Tharsis and Elysium and the polar layered terrains were formed (*46*). The absolute ages of these periods are not known but attempts have been made to estimate these by assuming that the martian cratering rate is some function of the lunar rate. Hartmann (*80*) suggested a rate of ~1.6 times the lunar rate, but this has been a matter of ongoing discussion for decades (*81–83*) and is further complicated by evidence—some of which is presented here as well as in (*84*)—for burial and exhumation of the craters that are usually counted in attempts to date surfaces. For the purposes of this work, and following the discussions of Tanaka (*47*), the Noachian is regarded here to have occurred before 3.5 billion years ago, and the Amazonian, after anywhere from ~3.5 to 1.8 billion years ago.
3. J. B. Pollack *et al.*, *Icarus* **71**, 203 (1987).
4. S. W. Squyres, J. F. Kasting, *Science* **265**, 744 (1994).

5. J. F. McCauley, *U.S. Geol. Surv. Misc. Inv. Ser. Map I-897* (1978).
6. S. S. Nedell *et al.*, *Icarus* **70**, 409 (1987).
7. S. W. Squyres, *Icarus* **79**, 229 (1989).
8. G. Komatsu *et al.*, *J. Geophys. Res.* **98**, 11105 (1993).
9. N. A. Cabrol, E. A. Grin, *Icarus* **142**, 160 (1999).
10. C. P. McKay, C. R. Stoker, *Rev. Geophys.* **27**, 189 (1989).
11. J. F. Kerridge *et al.*, Eds., *NASA Spec. Publ., NASA SP-530*, 1995.
12. J. D. Farmer, D. J. Des Marais, *J. Geophys. Res.* **104**, 26977 (1999).
13. The units we describe are not the first layered materials to be recognized on Mars. Before MGS, layered accumulations—including some of several kilometers thickness—were found at the two martian poles [thought to be a mixture of silicate dust and ice (*85*)]. Other known layered features include the Medusae Fossae Formation west of Tharsis (*86*), the walls and the interior layered mesas of the Valles Marineris (*87*), exposures in the upper walls of Kasei Valles (*88*), and within Terra Meridiani (*89*).
14. Mantles are defined here as surficial sedimentary deposits of smooth texture (at spacecraft image pixel scales of 1.5 to 20 m) and locally uniform thickness that appear to drape all but the steepest topography. Mantles show morphologies similar to terrestrial loess and primary air fall tephra deposits. Unlike dunes or thick sand sheets, mantles do not appear to have involved ground transport and interaction with local topography. Mantles are generally thought to have been emplaced by settling after transport by suspension in the atmosphere (*90*).
15. "Unit" is a nongenetic term for a surface, bed, layer, or group of materials that share common attributes; a unit may be seen in section in a cliff or as adjacent surface expressions of underlying materials, but surface expression does not imply a stratigraphic relation, nor vice versa. A "deposit" is a unit for which processes of sedimentation have been demonstrated or inferred to have operated, specifically, for which evidence that material has been imported and laid down on the surface.
16. "Tone" describes the brightness of a material relative to other features seen by the MOC and to the overall range of martian surface brightness (excluding the polar caps). A feature is described as light-toned if it is relatively bright, dark if it has a qualitatively low albedo, and intermediate if the tone is neither dark nor light. Quantitative albedo cannot be extracted from MOC images; however, units in Terra Meridiani are large enough that albedos derived from 60-km-binned Viking Infrared Thermal Mapper observations (*91*) suggest that light-toned units have albedos of >0.22 and dark-toned units have albedos typically of <0.15.
17. In the absence of precise topographic information, qualitative assessments of layer thickness are applied. Because the apparent thickness of a layer can be affected by slope (a thick unit may appear as a thin band in an overhead view if it is expressed on a steep slope), photometric shading and true shadowing are also used in assessing thickness. A thin unit, subunit, bed, or layer is one that subtends only a few picture elements on flat or relatively low slopes.
18. Geologic relations are determined through application of the principle of photographic interpretation to images acquired by the MOC. Seven attributes of the geology are used: planimetric configuration (the two-dimensional shape of features), relief (topography, determined by shading or parallax), brightness, color, texture (the aggregate appearance of small features), pattern (the aggregate appearance of large features), and context (the relation of features to one another).
19. There is no evidence to suggest that apparently identical sequences found in widely separated locations are in fact the same materials from the same sources deposited at the same time in the same sequence, and this interpretation is not advocated here.
20. Massive unit examples are common in Ganges Chasma (e.g., MOC image M04-00323), Hebes Chasma (e.g., M09-00284), and eastern Candor Chasma (e.g., M02-00832).
21. K. S. Edgett, M. C. Malin, *Lunar Planet. Sci.* **XXXI** (abstr. 1057) (2000) [CD-ROM].
22. C. K. Wentworth, *J. Geol.* **30**, 377 (1922).
23. Large boulders at the base of cliffs are common in volcanic regions on Mars but are much less common in nonvolcanic terrain. Examples can be seen in the Olympus Mons caldera (e.g., MOC images M07-04611, M12-01922, and M13-01049).
24. J. F. McCauley *et al.*, *U.S. Geol. Surv. Interagency Rep., Astrogeol. 81* (1977).
25. R. P. Sharp, *J. Geol.* **71**, 617, 1963.
26. Examples include beds in the far west-northwest region of Candor Chasma (e.g., MOC image FHA-01279), seen to be dipping to the east, and in a crater at 8°N, 7°W (e.g., image M14-01647), where they are superimposed on the northern wall of the crater and dip toward the south.
27. Maps of planetary surfaces, although traditionally called geologic maps, mostly show relations inferred from morphology. Following Shoemaker and Hackman (*92*), such maps portray planar surfaces (produced by volcanism or planet-wide emplacement of impact ejecta blankets in the original case of the moon) and the superposition onto these plains, or the embayment by these plains, of local or regional impact crater ejecta. Rock and time stratigraphic relations are considered equivalent. As applied to Mars, these techniques were expanded to describe geomorphic landforms by arguing that their surfaces were materials whose ages reflected the processes that created the landforms (*93*). The primary focus is to place features within the planet-wide chronology established through crater counting. Although we cannot determine the composition of the outcrop materials described herein and must infer their age from relative relations, the MOC data, especially when combined with MGS laser altimetery, allow terrestrial-style geologic maps of portions of Mars to be rendered by virtue of their ability to reveal the tops, bottoms, and lateral extents of actual rock units.
28. Detailed unit descriptions for the Gale Crater geologic map have been submitted for publication (K. S. Edgett, M C. Malin, in preparation). An electronic copy of the abstract is available from the authors at www.msss.com/gale.pdf.
29. Some layered outcrops occur at latitudes poleward of 30°; examples include a mound in Galle Crater at 52.2°S, 30°W (e.g., MOC images M04-00129, M14-02055, M15-01649, and M18-01719) and an outcrop in Spallanzani Crater at 58.3°S, 273.3°W (M02-03885).
30. "Intercrater plains" are rolling to smooth surfaces between craters within regions of martian highland terrain characterized by the occurrence of many large (>25 km diameter) impact craters.
31. K. S. Edgett, M. C. Malin, *Lunar Planet. Sci.* **XXXI** (abstr. 1066) (2000) [CD-ROM].
32. The contact between the thin mesa unit that correlates with the MGS TES observation of hematite (*33*) and the underlying light-toned layered units is interpreted by us to be an unconformity on the basis of examining laser altimeter topographic profiles and MOC images together. These show that the unit is thin with light-toned outcrops exposed in windows through areas where the unit is thinnest (e.g., raw decompressed MOC image M09-00545 at line 4645, sample 300), but the underlying topography varies by hundreds of meters over tens of kilometers independent of the thickness of the "hematite" thin mesa unit.
33. P. R. Christensen *et al.*, *J. Geophys. Res.* **105**, 9623 (2000).
34. Example MOC images in the Mawrth Vallis region are M02-00805, M03-00921, M03-01810, and M04-00781.
35. Example MOC images in Aeolis region: M07-02180, M07-05032, M09-06064, and M11-02277.
36. Example MOC images in northeast Hellas rim region are M00-01300, M03-01307, and M10-03400.
37. R. P. Sharp, *J. Geophys. Res.* **78**, 4073 (1973).
38. Aram Chaos is located at 2.8°N, 21.2°W. Example MOC images that show outcrop materials are M04-03228, M11-02955, M12-01687, and M19-00766.
39. Iani Chaos is located at 1.7°S, 18.2°W. Example MOC images that show outcrop materials are M03-01804, M11-01182, M13-01484, and M20-01046.
40. Examples of light-toned layered and massive outcrops in the walls of the Valles Marineris are seen in: (i) west Candor Chasma in MOC images M17-00467 (in Fig. 12) and M20-01506; (ii) ridges in Coprates Chasma in images M20-00380, M20-01760, and M21-00103; and (iii) Ius Chasma in image M08-07173.
41. Layered units in west Candor Chasma are best seen going into and under the chasm walls in images M14-00631, M18-00099, and M19-00784.
42. Use of the term "rock" is somewhat of a semantic issue. We use this term because the outcrop materials exhibit the variety of properties common to terrestrial layered rock outcrops. Thermophysical properties estimated from Phobos 2 Termoskan and TES observations suggest that larger exposures, such as the light-toned intracrater outcrops of Terra Meridiani and the layered material in the Valles Marineris, have an elevated thermal inertia consistent with the presence of unconsolidated coarse-grained material, but none of these observations have spatial resolution sufficient to see the thermal signature of solid rock if the rock is not cleanly exposed at the scales of 2 to 5 km (*94*, *95*).
43. The presence of layering indicates change. In general, a layer is a record of similarity and the upper and lower boundaries record instability; repetitious layering indicates repeated or episodic changes. Such layering can be either irregular or regular. Irregular but repetitious layering usually indicates a system that is neither forced, damped, nor harmonic. Variations (changes) cannot be correlated from one position in a sequence to another, other than by the simplest of relations—the higher layer is younger.
44. Alternatively, the lack of craters might indicate that (i) they do not retain craters (unlikely, given the evidence that they maintain topographic and stratigraphic attributes); (ii) the materials are easily and quickly eroded (also unlikely, but perhaps less so, as they have sufficient strength to retain near-vertical slopes); or (iii) impact craters never formed on these surfaces (unlikely, but remotely possible).
45. Hartmann *et al.* (*96*, *97*) obtain ages of ≤100 million years for what have been interpreted to be among the youngest volcanic surfaces on Mars, yet these surfaces are 10 to 100 times more cratered than any of the layered or massive units at the locations in Fig. 2.
46. D. H. Scott, M. H. Carr, *U.S. Geol. Surv. Misc. Inv. Ser. Map I-1083*, scale 1:15,000,000 (1978).
47. K. L. Tanaka, *Proc. Lunar Planet. Sci. Conf. 17th*, part 1, *J. Geophys. Res.* **91** (suppl.), E139 (1986).
48. A. S. McEwen *et al.*, *Nature* **397**, 584 (1999).
49. This interpretation is a radical departure from the prevailing, pre-MGS view that the layered and massive units in the Valles Marineris are Hesperian and Amazonian in age and were deposited after the troughs opened (*98*); however, it is the only interpretation that can explain outcrops in and under the chasm walls.
50. For the purposes of this discussion, we assume for subaqueous cases that the transport medium was water, taking our cue from research reported in hundreds of papers written since the observation of valleys and channels in Mariner 9 images—that water was the most likely agent of erosion of such features on Mars.
51. We emphasize pyroclastic materials because they share many of the characteristics of sediment and because pyroclastic eruptions are known to create layered and massive units in close proximity and with specific stratigraphic relations in some ways resembling those seen on Mars (*99*). With regard to other volcanic products (flows), we note that the physical properties of and relative stratigraphic relations within the martian outcrop materials are unlike those of terrestrial effusive basaltic lava flows. Cliffs in volcanic regions on Mars shed boulders (*23*), whereas the layered, massive, and thin mesa outcrops rarely shed boulders, even on steep slopes. The upper surfaces of individual layers in the martian outcrops, as exposed by layer retreat, are flat and smooth, whereas areally extensive lava flows elsewhere on Mars tend to have rugged, platy and pressure-ridged upper surfaces (*100*).

52. R. P. Sharp, M. C. Malin, *Geol. Soc. Am. Bull.* **86**, 593 (1975).
53. D. C. Pieri, *Icarus* **27**, 25 (1976).
54. M. C. Malin, M. H. Carr, *Nature* **397**, 589 (1999).
55. M. H. Carr, M. C. Malin, *Icarus* **146**, 366 (2000).
56. D. L. Blaney, T. B. McCord, *J. Geophys. Res.* **94**, 10159 (1989).
57. P. R. Christensen *et al.*, *Science* **279**, 1692 (1998).
58. J. R. Zimbelman, *Lunar Planet. Sci.* **XXI**, 1375 (1990).
59. R. B. Leighton *et al.*, *Science* **149**, 627 (1965).
60. E. J. Öpik, *Ir. Astron. J.* **7**, 473 (1965).
61. W. K. Hartmann, *Icarus* **5**, 565 (1966).
62. ———, *Icarus* **15**, 410 (1971).
63. C. R. Chapman *et al.*, *Astron. J.* **74**, 1039 (1968).
64. L. A. Soderblom *et al.*, *Icarus* **22**, 239 (1974).
65. W. K. Hartmann, *J. Geophys. Res.* **78**, 4096 (1973).
66. K. L. Jones, *J. Geophys. Res.* **79**, 3917 (1974).
67. C. R. Chapman, *Icarus* **22**, 272 (1974).
68. R. A. Craddock, T. A. Maxwell, *J. Geophys. Res.* **95**, 14265 (1990).
69. ———, *J. Geophys. Res.* **98**, 3453 (1993).
70. Malin (*84*) considered the oldest terrain on Mars as cratered "volumes" rather than as cratered "surfaces," with craters formed over a period of time while deposition was occurring simultaneously. In such locations, the rim relief of a large crater might stick up through several younger layers, whereas some nearby smaller craters of comparable age might be buried, others might be exhumed, and still others, substantially younger than any of their neighbors, might also be visible.
71. M. C. Malin *et al.*, *Science* **279**, 1681 (1998).
72. M. C. Malin, K. S. Edgett, *Fifth International Conference on Mars* (abstr. 6027) (Lunar and Planetary Institute, Houston, TX, 1999) [CD-ROM].
73. R. B. Leighton, B. C. Murray, *Science* **153**, 136 (1966).
74. F. P. Fanale, *Icarus* **28**, 179 (1976).
75. Such variations have most often been invoked as the explanation for the repetitively layered polar materials.
76. W. R. Ward, *J. Geophys. Res.* **79**, 3375 (1974).
77. ——— *et al.*, *J. Geophys. Res.* **79**, 3387 (1974).
78. O. B. Toon *et al.*, *Icarus* **44**, 552 (1980).
79. M. C. Malin *et al.*, *J. Geophys. Res.* **97**, 7699 (1992).
80. W. K. Hartmann, *Meteorit. Planet. Sci.* **34**, 167 (1999).
81. G. Neukum, D. U. Wise, *Science* **194**, 1381 (1976).
82. G. Neukum, K. Hiller, *J. Geophys. Res.* **86**, 3097 (1981).
83. W. K. Hartmann *et al.*, in *Basaltic Volcanism on the Terrestrial Planets* (Pergamon, New York, 1981), pp. 1050–1129.
84. M. C. Malin, thesis, California Institute of Technology, Pasadena (1976), chap. 3.
85. J. A. Cutts, *J. Geophys. Res.* **78**, 4231 (1973).
86. D. H. Scott, K. L. Tanaka, *U.S. Geol. Surv. Misc. Inv. Ser. Map I-1802-A* (1986).
87. K. R. Blasius *et al.*, *J. Geophys. Res.* **82**, 4067 (1977).
88. K. L. Tanaka, M. G. Chapman, *Proc. Lunar Planet. Sci.* **22**, 73 (1992).
89. K. S. Edgett, T. J. Parker, *Geophys. Res. Lett.* **24**, 2897 (1997).
90. P. R. Christensen, *J. Geophys. Res.* **91**, 496 (1986).
91. ———, *J. Geophys. Res.* **93**, 7611 (1988).
92. E. M. Shoemaker, R. J. Hackman, in *The Moon: Symposium 14*, Z. Kopal, Z. K. Mikhailov, Eds. (Academic Press, New York, 1962), pp. 289–300.
93. D. E. Wilhelms, in *Planetary Mapping*, R. Greeley, R. M. Batson, Eds. (Cambridge Univ. Press, New York, 1990), pp. 208–260.
94. A. S. Selivanov *et al.*, *Nature* **341**, 593 (1989).
95. M. T. Mellon *et al.*, *Icarus*, in press.
96. W. K. Hartmann *et al.*, *Nature* **397**, 586 (1999).
97. W. K. Hartmann, D. C. Berman, *J. Geophys. Res.* **105**, 15011 (2000).
98. B. K. Lucchitta *et al.*, in *Mars*, H. H. Kieffer *et al.*, Eds. (Univ. of Arizona Press, Tucson, AZ, 1992), pp. 453–492.
99. R. V. Fisher, H.-U. Schmincke, *Pyroclastic Rocks* (Springer-Verlag, Berlin, 1984).
100. L. Keszthelyi, *et al.*, *J. Geophys. Res.* **105**, 15027 (2000).
101. We thank J. Garvin for assistance with laser altimeter data and thoughtful input from two anonymous referees. We thank D. Michna, M. Caplinger, E. Jensen, S. Davis, W. Gross, K. Supulver, J. Warren, R. Adair, J. Sandoval, L. Posiolov, R. Zimdar, and M. Ravine for operational support; we also express our appreciation to the MOC Science Team for their patience. Supported by the National Aeronautics and Space Administration through contract 959060 from the Jet Propulsion Laboratory.

25 September 2000; accepted 13 November 2000

Planar Hexacoordinate Carbon: A Viable Possibility

Kai Exner and Paul von Ragué Schleyer*

The viability of molecules with planar hexacoordinate carbon atoms is demonstrated by density-functional theory (DFT) calculations for CB_6^{2-}, a CB_6H_2 isomer, and three C_3B_4 minima. All of these species have six π electrons and are aromatic. Although other C_3B_4 isomers are lower in energy, the activation barriers for the rearrangements of the three planar carbon C_3B_4 minima into more stable isomers are appreciable, and experimental observation should be possible. High-level ab initio calculations confirm the DFT results. The planar hexacoordination in these species does not violate the octet rule because six partial bonds to the central carbons are involved.

Saturated carbon is usually tetrahedrally coordinated, and planar arrangements were long thought to be too high in energy to be observed. Nevertheless, experimental evidence for planar tetracoordinate carbon species predicted by theory (*1–5*) continues to accumulate (*3*, *6–9*). Nonetheless, planar arrangements with six atoms bound to carbon seem impossible. Many known compounds have hexacoordinate carbons (Fig. 1) (*10–18*), but they are involved in three-dimensional structures.

Are planar hexacoordinate arrangements really inconceivable? The design of unusual molecular shapes requires the right "fit" of the constituent atoms, both geometrically and electronically (*3*). The interatomic distances must be in the normal ranges. The molecular orbital (MO) patterns and degeneracies should be consistent with the molecular symmetry. In addition, the occupied orbitals should be low in energy and doubly occupied (*1*, *3*, *19*). Unusually high coordination of a central atom can best be achieved in cyclic systems or clusters in which all atom-atom contacts are bonding.

Our interest in planar hexacoordinate carbon was triggered by nucleus-independent chemical shift (NICS) evaluations of aromaticity (*20–22*). NICS values are based on magnetic shieldings computed by means of "ghost atoms" (designated points in space) positioned, for example, in the center of the benzene ring. We wondered whether such surrogate probes could be replaced by a carbon atom or ion. If the cyclic electron delocalization is retained, the aromatic stabilization energy might help support unusual coordination of the central carbon. We now report an exploration of several candidates with carbon in the center of a six-membered ring using density-functional theory (DFT) calculations (B3LYP/6-311+G**) (*23*).

It is not surprising that neutral atoms do not fit in the center of benzene. Very high energy (244 kcal mol^{-1}) is needed to force helium (the smallest atom) to pass through the benzene plane [$He@C_6H_6$ with hexagonal planar geometry (D_{6h} symmetry) is a transition state with bond lengths $r_{CC} = r_{CHe} = 1.517$ Å]. The situation with a central carbon is even worse because the larger atomic radius and its excess valence electrons are unsupportable. Indeed, we could not optimize neutral C_7H_6 when D_{6h} symmetry was imposed; even the Jahn-Teller–distorted D_{2h} form (**9**) (Fig. 2) was highly unstable, having 11 imaginary frequencies (an equilibrium structure has none) (*24*). D_{6h} optimization was possible after the removal of two electrons. The resulting $C_7H_6^{2+}$ dication has a structure with 1.601 Å carbon-carbon bond lengths, but there are eight imaginary frequencies. The D_{6h} tetracation $C_7H_6^{4+}$ (**10**), which can be imagined as a valence electron–stripped carbon atom inserted into benzene, has more realistic carbon-carbon bond lengths ($r_{CC} = 1.516$ Å), but it is still characterized by two imaginary frequencies. The

Center for Computational Quantum Chemistry, Computational Chemistry Annex, University of Georgia, Athens, GA 30602–2525, USA.

*To whom correspondence should be addressed. E-mail: schleyer@chem.uga.edu